

Layered Double Hydroxide–CdSe Quantum Dot Composites through Colloidal Processing: Effect of Host Matrix–Nanoparticle Interaction on Optical Behavior

B. R. Venugopal,[†] N. Ravishankar,[‡] Christopher R. Perrey,[§] C. Shivakumara,^{||} and Michael Rajamathi^{*,†}

Department of Chemistry, St. Joseph's College, Lalbagh Road, Bangalore 560 027, India, Materials Research Center, Indian Institute of Science, Bangalore 560 012, India, Department of Chemical Engineering and Materials Science, University of Minnesota, Minneapolis, Minnesota 55455, and Solid State and Structural Chemistry Unit, Indian Institute of Science, Bangalore 560 012, India

Received: August 24, 2005; In Final Form: November 12, 2005

Layered double hydroxide (LDH)-monodispersed 4-nm CdSe nanoparticle composites were prepared through restacking of layers of colloiddally dispersed delaminated LDH in the presence of CdSe nanoparticles in 1-butanol. The composites exhibit a blue shift for CdSe absorption, which increases with a decrease in nanoparticle content. The observed blue shift is due to the interaction of the quantum dots with the LDH layers, which leads to surface modification of the nanoparticles.

Introduction

Quantum dots (semiconductor nanoparticles) occupy the major part of current nanoparticle research due to their unique optical properties.^{1–3} Usually, the absorption edge of a semiconductor shifts toward blue upon decreasing the particle size^{4–6} because of the quantum size effect. Tuning the band gap of quantum dots is one of the fundamental interests in preparing novel materials. The band gap could be tuned either by changing the particle size^{4–8} or by altering the particle surface⁹ as surface defects play an important role in altering the band gap of semiconductor nanoparticles. It has also been shown that interaction with surrounding medium could also affect the optical behavior of semiconductor nanoparticles.¹⁰

Attempts have been made to prepare nanocomposites of quantum dots and inorganic hosts. For example, CdS nanoparticles have been grown in the pores of MCM-41 through intercalation of Cd²⁺ ions followed by reaction with H₂S.¹¹ Quantum dots have also been grown within the layers of layered hosts such as smectites,^{12–14} hydrotalcite,¹⁵ and K₂Ti₄O₉.¹⁶ The motivation behind the preparation of these composites has been to find applications in photocatalysis. In most of the reported work, a precursor is first intercalated within the layers and then it is converted into nanoparticles by a suitable posttreatment. In the typical method for the preparation of a smectite–nanoparticle composite, the smectite clay is first ion exchanged with the relevant metal ion and the exchanged solid is reacted with H₂S to form the metal sulfide nanoparticles in the interlayer region. In a slightly modified approach, Han et al.¹⁴ reported a single precursor method for synthesizing a CdS/montmorillonite nanocomposite by intercalating Cd[NH₂CSNH₂]₂Cl₂ into a clay host followed by hydrothermal decomposition. Optical properties of the composites have been studied in most of these cases, and the observed optical behavior has been attributed to particle

size effects even though there is no direct observation of particle sizes. The effect of host–nanoparticle interaction has not been studied in any of the reported work on these composites.

In all the existing methods, since quantum dots are grown within the layers, composites with uniformly sized nanoparticles may not be possible. We would not have any control over the growth of nanoparticles as it is affected by various factors such as the intercalation process, interaction between the precursor and host matrix, and the effect of posttreatment on the host lattice. In addition, in different compositions of the same composite, average particle size does not remain constant to help one understand the matrix–guest interaction. Typically, the particle size decreases with the decreased load of guest nanoparticles in the composite. Because of these reasons, there is a need for new approaches to the preparation of nanocomposites comprised of nanoparticles and layered solids where the size of the nanoparticles is uniform in a given composite and identical in all compositions of the same composite. Such composites can be prepared through colloidal processing.

Layered solids can be readily delaminated in solvents to get colloidal dispersions of monolayers, and the dispersed monolayers can be reassembled to form the parent layered solid. Almost all classes of layered solids have been shown to delaminate in aqueous and organic solvents through suitable manipulation of the interlayer region. Delamination of smectite clays,^{17,18} graphite oxide,^{19,20} metal phosphates,^{21,22} and layered double hydroxides^{23–26} (LDHs) have been well studied. We have been studying delamination of layered solids in organic media in recent times.^{26–28} By intercalating a suitable organophilic interlayer ion in a layered solid, we induce delamination and monolayer colloidal dispersion in organic solvents. The solvated monolayers could be reassembled through either evaporation or by changing the polarity of the medium. Capped nanoparticles can also be dispersed in organic solvents and reprecipitated by similar means. Using this behavior, one could easily build composites of layered solids and nanoparticles. In this work, we report the synthesis and optical behavior of LDH–semiconductor nanoparticle composites obtained by restacking

* To whom correspondence should be addressed. Tel: +91 80 2221 1429. Fax: +91 80 2224 5831. E-mail: mikerajamathi@rediffmail.com.

[†] St. Joseph's College.

[‡] Materials Research Center, Indian Institute of Science.

[§] University of Minnesota.

^{||} Solid State and Structural Chemistry Unit, Indian Institute of Science.

colloidally dispersed monolayers of an LDH in the presence of preformed, monodispersed, capped soluble nanoparticles of CdSe.

Experimental Section

Synthesis. LDH of the composition $Mg_2Al(OH)_6NO_3 \cdot 2H_2O$ (LDH–nitrate) was prepared using the procedure due to Olanrewaju et al.²⁹ A mixture of solutions of $Mg(NO_3)_2 \cdot 6H_2O$ and $Al(NO_3)_3 \cdot 9H_2O$ in the molar ratio 2:1 was added dropwise into a 1 M solution of NH_4OH with constant, vigorous stirring. After the addition was complete, the resultant white slurry was aged at 65 °C overnight. The solid product obtained was washed free of ions with decarbonated water followed by acetone and dried at 65 °C in an air oven to constant weight.

To get the dodecyl sulfate (DS), a surfactant, intercalated LDH referred to as LDH–DS here afterward, 3.32 mmol (1 g) of LDH–nitrate was stirred with 18.92 mmol (5.5 g) of sodium dodecyl sulfate (SDS) dissolved in 35 mL of decarbonated water for 8 days in a sealed container. The product obtained was washed with copious amounts of decarbonated water followed by acetone and dried at 65 °C in an air oven to constant weight.

Dodecanethiol-capped 4-nm monodisperse CdSe nanoparticles were prepared as described by Gautam et al.³⁰ Amounts of 1.36 g of cadmium stearate, 0.158 g of selenium powder, 0.2 g of tetralin, and 0.1 g of dodecanethiol were taken in 50 mL of toluene in a Teflon gasketed stainless steel bomb (~70% filling). The bomb was held at 250 °C for 5 h and cooled to room temperature. The transparent red solution obtained was treated with 2-propanol to precipitate CdSe nanoparticles. The product was redissolved in toluene and precipitated again using 2-propanol. This procedure was repeated four times to get nanoparticles of identical particle size.

CdSe nanoparticles were dispersed in 1-butanol by sonicating at ~70 °C for 2 h. Similarly, LDH–DS was delaminated and dispersed in 1-butanol under identical conditions. Both the colloids were mixed in different proportions and sonicated for an additional hour. Composites recovered by evaporating the solvent at ~100 °C were washed repeatedly with acetone and dried in an air oven at 65 °C to constant weight. The mass ratios m_{CdSe}/m_{LDH} in the composites were 1:100, 3.5:100, 5:100, 10:100, and 25:100.

To study the effect of the high-temperature treatment and sonication during the composite preparation on CdSe nanoparticles, a part of the nanoparticle sample was sonicated in 1-butanol for 3 h and the resultant colloid was evaporated at 100 °C and the resultant product, the heat-treated CdSe nanoparticle, was compared with as-prepared CdSe.

Characterization. The powder X-ray diffraction (pXRD) patterns of the materials were recorded on a Philips X'Pert Pro diffractometer fitted with a secondary graphite monochromator. $Cu K\alpha$ radiation with $\lambda = 1.5418 \text{ \AA}$ was used. Data were collected at the rate of 2° per minute over the 2θ range of 2–65°. Infrared spectra were obtained from a Nicolet Model Impact 400D FTIR spectrometer with 4 cm^{-1} resolution. Sample pellets were made by pressing a mixture of the sample and KBr in the required ratio. Transmission electron microscopic (TEM) investigations were carried out using a JEOL 200CX instrument operated at 160 kV. High-resolution electron microscopic (HREM) studies were carried out using a TECNAI F30 electron microscope operated at 300 kV. UV–vis absorption spectra of powder samples were recorded in reflectance mode using a Perkin-Elmer Lambda 35 spectrometer.

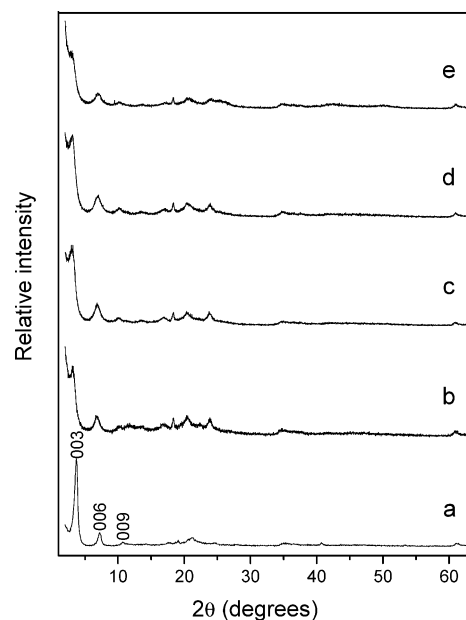


Figure 1. Powder X-ray diffraction patterns of LDH–DS (a) and the LDH–CdSe composites of the composition $m_{CdSe}/m_{LDH} = 1:100$ (b), 3.5:100 (c), 5:100 (d), and 10:100 (e).

Results and Discussion

In Figure 1, we compare the pXRD patterns of the composites with those of the matrix LDH–DS. The first peak with the d spacing of 23.9 Å of the LDH–DS (Figure 1a) suggests that the alkyl chains of DS lie almost parallel to the c -axis with the alkyl chains of the adjacent layers interpenetrating each other. The basal spacing of the LDH depends on the nanoparticle content in the composite. It increases from 23.9 to 27.6 Å for a 1:100 composite (Figure 1b) and reaches a value of 30.1 Å for a 10:100 composite (Figure 1e). The fact that the increase in interlayer spacing is dependent on the nanoparticle content suggests that the observed interlayer expansion is not brought about by intercalation of solvent molecules. In all the composites, the $00l$ reflections are quite broadened. For example, the full width at half maximum (fwhm) of the 006 reflection of the parent LDH–DS is 0.58°, while it increases to 0.85° in the 1:100 composite and it steadily increases with the nanoparticle load to reach a value of 1.10° for the 10:100 composite. This indicates that the nanoparticles are partially intercalated in the layered solid. Only partial intercalation is expected, as the nanoparticle contents in the composites are insufficient for complete intercalation. Partial intercalation would lead to a structure similar to interstratified structures³¹ with the basal spacing being the weighted average of spacings from the intercalated and unintercalated regions. The possibility of the presence of a physical mixture of LDH–DS crystallites and CdSe nanoparticles may be ruled out from the observation that the basal spacing and the peak broadening of the $00l$ reflections of the composites increase with an increase in the load of nanoparticles in the composite. If the composites were only physical mixtures, then the basal spacing should have remained 23.9 Å in all the composites and the $00l$ reflections should not have been broadened at all or broadened to the same extent in all the composites.

To confirm that the nanoparticles are indeed incorporated in the interlayer region of the host, we prepared a composite with an excess of nanoparticles. In Figure 2, we compare the low-angle XRD of the composites. While the composites with lower loads of nanoparticles (parts a and b of Figure 2) exhibit their

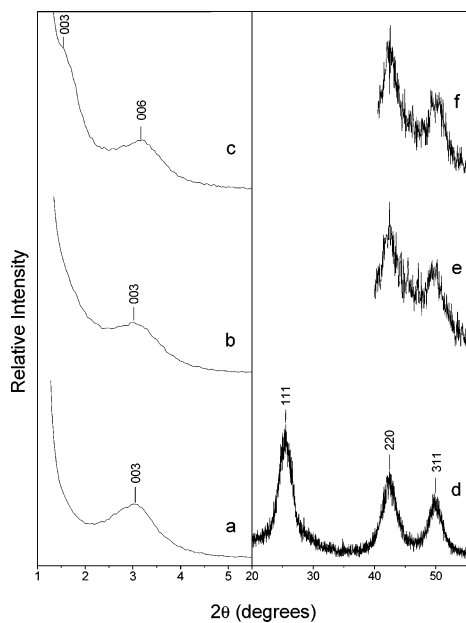


Figure 2. Left panel shows the low angle X-ray diffraction patterns of LDH–CdSe composites of the composition $m_{\text{CdSe}}/m_{\text{LDH}} = 5:100$ (a), 10:100 (b), and 25:100 (c). The right panel compares the X-ray diffraction pattern of the free CdSe nanoparticles (d) with the relevant regions of the diffraction patterns of the composites of composition $m_{\text{CdSe}}/m_{\text{LDH}} = 10:100$ (e) and 25:100 (f).

first reflection at around 3° similar to the parent LDH–DS (Figure 1a), the composite with $m_{\text{CdSe}}/m_{\text{LDH}} = 25:100$ (Figure 2c) shows its first reflection at $2\theta = 1.6^\circ$ corresponding to a basal spacing of $\sim 56 \text{ \AA}$ due to a complete intercalation of the nanoparticles in the interlayer region.

The pXRD pattern of dodecanethiol-capped CdSe nanoparticles (Figure 2d) is similar to that reported by Gautam et al.³⁰ and indicates a cubic zinc blende structure for the particles as shown by these authors through simulation studies. A small region of the XRD patterns of the composites shown in parts e and f of Figure 2 shows two peaks corresponding to the (220) and (311) reflections of the CdSe nanoparticles. The nature of these reflections in the composite remains almost identical to that of the free nanoparticles suggesting that the nanoparticles have the same structure, size, and shape in the composites.

The IR spectra of the composites are compared with those of the LDH–DS host and the CdSe nanoparticles in Figure 3. In the host LDH–DS, DS are the only interlayer ions as confirmed by the absence of the nitrate absorption peak around 1381 cm^{-1} or carbonate absorption peak around 1364 cm^{-1} in the IR spectrum (Figure 3a). The broad and sharp absorption around 1180 cm^{-1} in Figure 3a corresponds to the S=O stretching vibration of the sulfate group of DS. The strong absorptions at 2857, 2930, and 2960 cm^{-1} can be attributed to the C–H stretching vibrations of the alkyl chains of DS, whose nature suggests that the alkyl chains take up an all-trans conformation.^{32,33} The presence of the capping agent, dodecanethiol, in the CdSe nanoparticle is confirmed by the presence of sharp C–H stretching vibrations around 2860, 2930, and 2960 cm^{-1} (Figure 3b). Here again, the alkyl chains take up an all-trans conformation.³⁰ The IR spectrum of the 1:100 composite (Figure 3c) shows features of both the host LDH–DS and the CdSe nanoparticles. However, the C–H stretching absorptions are slightly modified in intensity indicating conformational changes arising from the interaction of the alkyl chains of the capping agent molecules with the alkyl chains of the interlayer surfactant ions. The IR spectrum of the 25:100 composite

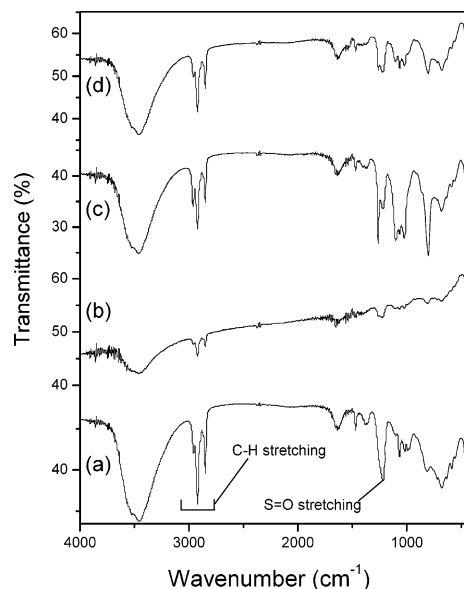


Figure 3. IR spectra of LDH–DS (a), CdSe nanoparticles (b), LDH–CdSe composites of the composition $m_{\text{CdSe}}/m_{\text{LDH}} = 1:100$ (c), and 25:100 (d).

(Figure 3d) shows features similar to the 1:100 composite with only a variation in intensity arising out of the lower load of the host matrix.

The TEM image of the CdSe particles shown in Figure 4a indicates that the sample is made of almost uniform 4-nm spherical particles. Low-magnification TEM images of two of the composites (5:100 and 10:100) are shown in parts b and c of Figure 4. The dark regions indicate the presence of the particles. The darker contrast is due to the higher mass thickness in those regions as the average atomic number of the nanoparticle is higher than that of the matrix. The image also indicates that the particles are distributed uniformly in the composite. The inset in Figure 4b is a selected area diffraction pattern showing the (220) and (311) rings from the cubic CdSe phase. Figure 4d is a higher magnification image of the 5:100 composite showing a set of larger fringes along with another set of underlying lattice fringes of the nanoparticles distributed through the entire composite. For the most part, the larger fringes show varied distances of 1.4–1.6 nm which cannot be attributed to the LDH–DS layers as it has an interplanar distance of 2.39 nm in the unintercalated state and which should be even more in the nanoparticle intercalated state. Thus, we assume these fringes to be Moiré fringes arising from the interaction of intercalated and unintercalated crystallites of the LDH or the interaction of the LDH crystallites and the nanocrystals. The underlying finer fringes, which are about 0.35 nm, are due to the nanoparticles. The average extent of a particular set of underlying finer fringes is of the order of 4 nm, which is in agreement with the particle size of the free CdSe nanoparticles. This confirms that the particle size of the nanoparticles remains unaffected in the composites.

In Figure 5, we show the UV–vis absorption spectra of the host LDH–DS, free CdSe nanoparticles, and the composites. The host solid (Figure 5a) has no absorption in the region studied. CdSe nanoparticles (Figure 5b) show an absorption maximum at 576 nm with the band gap energy (E_g) calculated from the band edge being 2.071 eV. The slope of the band edge is quite high, indicating monodispersity. The composites (parts d–h of Figure 5) show a blue shift in the absorption maximum and the band gap of the CdSe particles. The extent of the shift increases with a decrease in the nanoparticle content in the

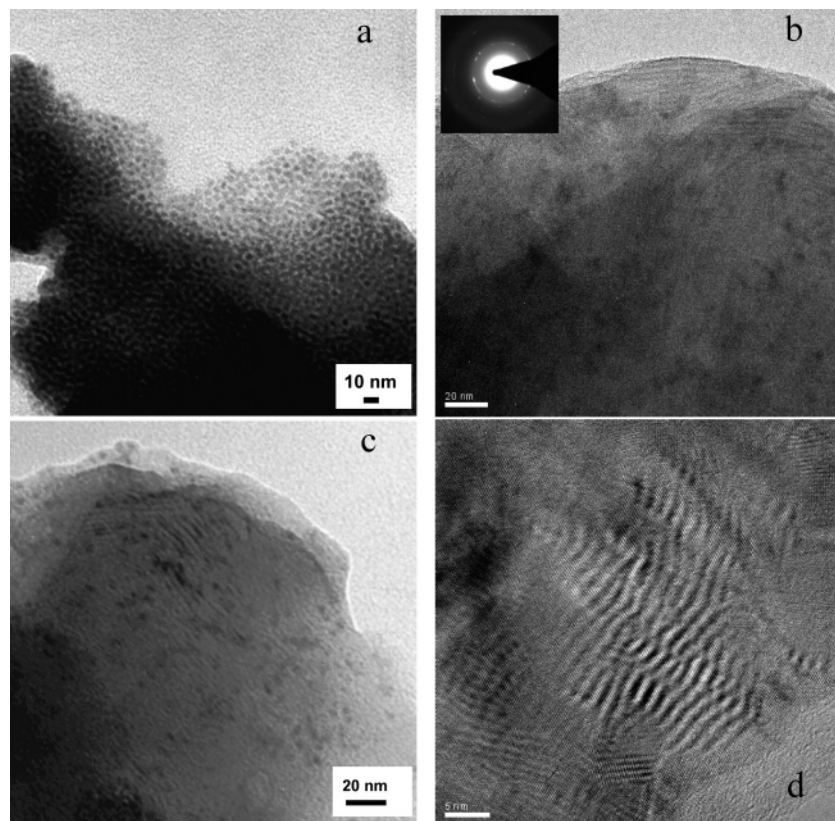


Figure 4. Low-resolution image showing CdSe nanoparticles of the order of 4 nm (a), bright field images from the 5:100 (b), and 10:100 (c) composites showing uniform distribution of particles in the matrix. The inset in (b) shows the diffraction pattern from the composite showing 220 and 311 rings from the cubic CdSe phase. (d) High-resolution image of the composite showing extensive Moiré fringes.

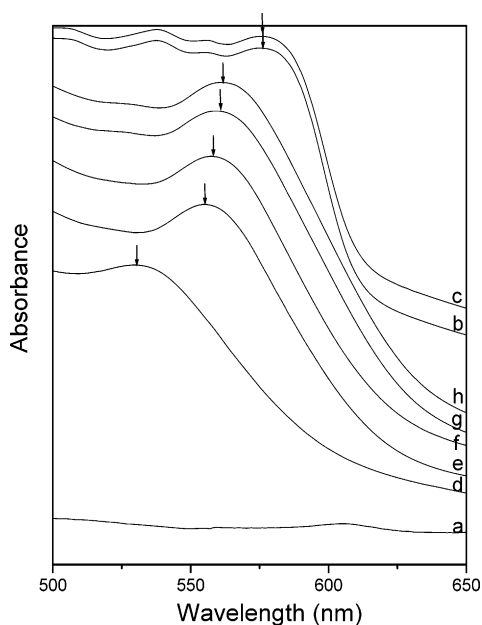


Figure 5. UV-vis absorption spectra of LDH–DS (a), free CdSe nanoparticles (b), heat-treated CdSe nanoparticles (c) along with the composites of the composition $m_{\text{CdSe}}/m_{\text{LDH}} = 1:100$ (d), 3.5:100 (e), 5:100 (f), 10:100 (g), and 25:100 (h). Arrows indicate the absorption maxima.

composite as listed in Table 1. While the absorption maximum for the free CdSe nanoparticles is 576 nm, it is decreased to 562 nm in the 25:100 composite. As the CdSe load decreases, the absorption maximum decreases steadily to reach the value of 531 nm in the 1:100 composite. The band gap of the particles in the composites also shows a similar trend. While it is 2.071

TABLE 1: Absorption Maxima and E_g of CdSe Nanoparticles Compared with Those of the Composites

sample	absorption maxima (nm)	E_g (eV)
free CdSe nanoparticles	576	2.071
heat-treated CdSe nanoparticles	576	2.071
25:100 composite	562	2.072
10:100 composite	561	2.074
5:100 composite	558	2.090
3.5:100 composite	555	2.102
1:100 composite	531	2.177

eV for free CdSe nanoparticles, it increases to 2.177 eV in the 1:100 composite.

The optical behavior of the composites can be explained as follows. The absorption maximum and E_g of the nanoparticles can be altered by changing the particle size, altering the surface of the particles, or by mere deaggregation. It could be argued that the size and shape of the particles could have been affected by processes such as oxidative etching due to the aggressive treatment—sonication and heating—during the preparation of the composites. However, free nanoparticles subjected to conditions identical to those employed during composite preparation—3 h of sonication and evaporation at 100 °C (heat-treated CdSe nanoparticles, Figure 5c)—show optical behavior identical to that of the starting CdSe particles (Figure 5b) suggesting that the CdSe particles do not change in size, shape, and dispersity during the composite preparation experiments. In addition, from the TEM images of the composites (Figure 4), it is obvious that the particle size of the CdSe nanoparticles in the composites is the same as that of the free particles.

The aggregation of semiconductor nanoparticles results in the delocalization of energy states, and this delocalization is lost when the sample is diluted in a matrix. Thus, dilution/

deaggregation itself can cause changes in optical behavior. However, from the reports available on polymer–nanoparticle composites, we see that the effect of deaggregation on the absorption maximum is not as pronounced as observed here. Artemyev et al.³⁴ report that the absorption maximum shifts toward blue by ~4 nm when the sample is highly diluted in a polymer matrix, whereas we observe a much larger blue shift, up to ~45 nm. Thus, we conclude that while a very small component of the blue shift of the absorption maxima could be due to dilution effects, the major contribution to the observed shifts comes from the host layer–nanoparticle interaction.

In all the composites, the absorption onset is more spread out with lower slopes compared to the free nanoparticles. This feature is common in dilute systems which has been observed in similar diluted composites of CdSe particles in the polymer matrix.³⁴

We ascribe the observed blue shifting of the absorption maximum in the LDH–nanoparticle composites to the surface modification of the particles affecting the density of the disordered states of the quantum dots arising from surface defects. To start with, the free CdSe particles show an increased E_g of 2.071 eV compared to bulk CdSe ($E_g = 1.84$ eV) as expected of small particles. The capping thiol molecules do not seem to reduce the surface defects very much as the observed E_g is quite low compared to what is reported for the 4-nm CdSe particles by others.³⁵ However, the matrix layers appear to be strongly interacting with the nanoparticles leading to the elimination of surface defects, which decreases the density of the disordered states. This leads to blue shifting of E_g as well as the absorption maximum in the composites. This interaction between the LDH–DS host and the nanoparticles increases with a decrease in the nanoparticle load in the composite. This allows us to tune the band gap and the absorption maximum of the CdSe nanoparticles. The fact that the optical behavior of the nanoparticles is affected in layered solid–nanoparticle composites even when the particle size remains constant suggests that the effects observed earlier in similar composites^{12–16} could be due to a combination of particle size effect and matrix–guest interactions.

Conclusions

Starting from preformed monodisperse nanoparticles and a delaminable layered solid we could obtain, through colloidal processing, LDH–nanoparticle composites in which the size of the nanoparticles remain uniform in composites of various composition. This procedure is quite general and can be adopted for the preparation of any layered solid–nanoparticle composite. The composites show different optical behavior even though the particle size of the nanoparticles remains constant. Thus, the observed changes in optical behavior are attributed to the layered host–nanoparticle interaction, which reduces the density of disordered states through surface passivation. We could tune the absorption maximum over a range of 45 nm by altering the composition of the composites.

Acknowledgment. This work was funded by DST, New Delhi. M.R. dedicates this work to Rev. Fr. J. C. Nelapaty.

References and Notes

- (1) Heath, J. R., Ed. *Acc. Chem. Res.* **1999**, *32*, 387.
- (2) Alivisatos, A. P. *Science* **1996**, *271*, 933.
- (3) Peng, X.; Manna, L.; Yang, W.; Wickham, J.; Scher, E.; Kadavanch, A.; Alivisatos, A. P. *Nature* **2000**, *404*, 59.
- (4) Brus, L. *J. Phys. Chem.* **1986**, *90*, 2555.
- (5) Weller, H.; Schmidt, H. M.; Koch, U.; Fojtik, A.; Baral, S.; Henglein, A.; Kunath, W.; Weiss, K.; Dieman, E. *Chem. Phys. Lett.* **1986**, *124*, 557.
- (6) Ekimov, A. I.; Efros, A. I.; Onushchenko, A. A. *Solid State Commun.* **1985**, *56*, 921.
- (7) Murry, C. B.; Norris, D. J.; Bawendi, M. G. *J. Am. Chem. Soc.* **1993**, *115*, 8706.
- (8) Jason Riley, D.; Waggett, J. P.; Upul Wijayantha, K. G. *J. Mater. Chem.* **2004**, *14*, 704.
- (9) Akamatsu, K.; Tsuruoka, T.; Nawafune, H. *J. Am. Chem. Soc.* **2005**, *127*, 1634.
- (10) Wang, Y.; Herroin, N. *J. Phys. Chem.* **1987**, *91*, 5005.
- (11) Zhang, Z.; Dai, S.; Fan, X.; Blom, D. A.; Pencycook, S. J.; Wei, Y. *J. Phys. Chem. B* **2001**, *105*, 6755.
- (12) Stramel, R. D.; Nakamura, T.; Thomas, J. K. *Chem. Phys. Lett.* **1986**, *130*, 423.
- (13) Enea, O.; Bard, A. J. *J. Phys. Chem.* **1986**, *90*, 301.
- (14) Han, Z.; Zhu, H.; Bulcock, S. R.; Ringer, S. P. *J. Phys. Chem. B* **2005**, *109*, 2673.
- (15) Sato, T.; Okuyama, H.; Endo, T.; Shimada, M. *React. Solids* **1990**, *8*, 63.
- (16) Shangguan, W.; Yoshida, A. *J. Phys. Chem. B* **2002**, *106*, 12227.
- (17) Lagaly, G. *Appl. Clay Sci.* **1999**, *15*, 1.
- (18) Fukushima, Y. *Clays Clay Miner.* **1984**, *32*, 320.
- (19) Matsuo, Y.; Hatase, K.; Sugie, Y. *Chem. Mater.* **1998**, *10*, 2266.
- (20) Matsuo, Y.; Tahara, K.; Sugie, Y. *Carbon* **1997**, *35*, 113.
- (21) Kim, H.-N.; Keller, S. W.; Mallouk, T. E.; Schmitt, J.; Decher, G. *Chem. Mater.* **1997**, *9*, 1414.
- (22) Alberti, G.; Cavalaglio, S.; Marmottini, F.; Matusek, K.; Megyeri, J.; Szirtes, L. *Appl. Catal., A* **2001**, *218*, 219.
- (23) Hibino, T.; Jones, W. *J. Mater. Chem.* **2001**, *11*, 1321.
- (24) Jobbagy, M.; Regazzoni, A. E. *J. Colloid Interface Sci.* **2004**, *275*, 345.
- (25) Adachi-Pagano, M.; Forano, C.; Besse, J.-P. *Chem. Commun.* **2000**, 91.
- (26) Venugopal, B. R.; Shivakumara, C.; Rajamathi, M. *J. Colloid Interface Sci.* **2006**, *294*, 234.
- (27) Rajamathi, J. T.; Ravishankar, N.; Rajamathi, M. *Solid State Sci.* **2005**, *7*, 195.
- (28) Nethravathi, C.; Harichandran, G.; Shivakumara, C.; Ravishankar, N.; Rajamathi, M. *J. Colloid Interface Sci.* **2005**, *288*, 629.
- (29) Olanrewaju, J.; Newalkar, B. L.; Mancino, C.; Komarneni, S. *Mater. Lett.* **2000**, *45*, 307.
- (30) Gautam, U. K.; Rajamathi, M.; Meldrum, F.; Morgan, P.; Seshadri, R. *Chem. Commun.* **2001**, 629.
- (31) Rajamathi, M.; Kamath, P. V.; Seshadri, R. *J. Mater. Chem.* **2000**, *10*, 503.
- (32) Snyder, R. G.; Strauss, H. L.; Elliger, C. A. *J. Phys. Chem.* **1982**, *86*, 5145.
- (33) MacPhail, R. A.; Strauss, H. L.; Snyder, R. G.; Elliger, C. A. *J. Phys. Chem.* **1984**, *88*, 334.
- (34) Artemyev, M. V.; Bibik, A. I.; Gurinovich, L. I.; Gaponenko, S. V.; Woggon, U. *Phys. Rev. B* **1999**, *60*, 1504.
- (35) Alivisatos, A. P.; Harris, A. L.; Levinos, N. J.; Steigerwald, M. L.; Brus, L. E. *J. Chem. Phys.* **1988**, *89*, 4001.